HYDROLOGICAL PROCESSES
Hydrol. Process. **24**, 160–169 (2010)
Published online 15 September 2009 in Wiley InterScience
(www.interscience.wiley.com) DOI: 10.1002/hyp.7434

Prediction of water table under stream–aquifer interactions over an arid region

Zhenghui Xie[1]* and Xing Yuan[1,2]

[1] *ICCES/LASG, Institute of Atmospheric Physics, Chinese Academy of Sciences, Beijing 100029, China*
[2] *Illinois State Water Survey, University of Illinois at Urbana–Champaign, Champaign 61820, USA*

Abstract:

In arid regions, groundwater is recharged laterally from rivers; this recharge is the primary source of water for vegetation. The rise or decline of the water table results in salinization or desertification respectively, and damages vegetation growth. Therefore, prediction of the water table with consideration of the stream–aquifer interactions is very important for understanding the hyporheic processes under human intervention, and to assess the ecological effects and water resource management of arid regions. This paper used a statistical-dynamical approach to predict the water table elevation near a river channel in an arid region from river discharge, which was achieved by a numerical model, a fitted stage-discharge function, and an automatic parameter calibration method. The model was established by reducing the problem of water table prediction under stream–aquifer interactions to an initial value problem of the differential equations with prescribed river discharge based on Darcy's law; the model parameters were automatically calibrated by the Shuffled Complex Evolution method. Synthetic experiments were used to test the sensitivities of the water table prediction to model parameters, and showed the robustness of the proposed scheme under different conditions. The proposed scheme was also calibrated and validated using data collected at the Yingsu section in the lower reaches of the Tarim River. The systematic biases, mean absolute errors, root mean squared errors, and correlation coefficients for the validation had ranges of $-0{\cdot}22 \sim 0{\cdot}16$ m, $0{\cdot}14 \sim 0{\cdot}33$ m, $0{\cdot}18 \sim 0{\cdot}44$ m and $0{\cdot}94 \sim 0{\cdot}99$ m respectively. Copyright © 2009 John Wiley & Sons, Ltd.

KEY WORDS water table; stream–aquifer interaction; stage-discharge; SCE-UA; Tarim River; arid region

Received 18 June 2008; Accepted 9 July 2009

INTRODUCTION

Groundwater, as a primary source, is essential for the economic development and sustaining of the ecosystem of arid regions such as the Tarim River basin in western China. The increased utilization of water resources and the arid climate of the river basin led to increased depth of the water table in the lower reaches of the Tarim River from 2–3 to 4–10 m during 1960–1980 (Feng *et al*., 2001). The deeper water table resulted in desertification and damaged vegetation growth (Hao *et al*., 2010). The ecological water conveyance project (EWCP) was implemented in 2000 to provide water to terrestrial ecosystems along the Tarim River. The EWCP transfers water from Bosten Lake to the Daxihaizi Reservoir, and finally to Taitema Lake (Xu *et al*., 2007). It is important to investigate the water table dynamics along the river channel including stream–aquifer interactions to assess the ecological effects of stream water conveyance and to manage water resources of arid regions.

Water table dynamics have been accounted for in several studies aiming to improve the land surface schemes and hydrological models (Liang *et al*., 2003; Yang and Xie, 2003; Maxwell and Miller, 2005; Yeh and Eltahir, 2005; Fan *et al*., 2007; Niu *et al*., 2007). These studies have focused on the large-scale variations in water table depths (Yuan *et al*., 2008a), the effects of the surface water and groundwater interactions on soil moisture, evaporation, recharge rate (Liang and Xie, 2003; Chen and Hu, 2004; Miguez-Macho *et al*., 2007; Wu *et al*., 2008), and even on regional climate (Anyah *et al*., 2008; Yuan *et al*., 2008b). Eco-hydrologists are interested in investigating the dynamical or statistical control processes of ecosystems by groundwater (Chen *et al*., 2004; Brolsma and Bierkens, 2007; Xu *et al*., 2007) and exchanges between near-channel and in-channel water (Sear *et al*., 1999; Sophocleous, 2002; Bauer *et al*., 2006; Chen, 2007; Hu *et al*., 2007), which are the key to evaluating the ecological structure of stream systems, and are critical to stream restoration and riparian management. Groundwater–river exchange can occur in either humid or arid climates (Figure 1a, b). In humid climates, the water table is normally maintained by precipitation at a higher-than-river level and therefore the groundwater discharges into the river, whereas in arid climates the water table is normally on a lower-than-river level and therefore the river recharges the aquifer. Some studies have calculated the lateral groundwater flow based on the differences between hydraulic heads of adjacent grid cells (Chen and Chen, 2003; Fan *et al*., 2007) and showed that hydraulic conductivity is one of the uncertainties in predicting water table using the head differences mechanism. Therefore, a robust

* Correspondence to: Zhenghui Xie, ICCES/LASG, Institute of Atmospheric Physics, Chinese Academy of Sciences, Beijing 100029, China. E-mail: zxie@lasg.iap.ac.cn

auto-calibration method should be introduced to make full use of the available data and enhance model performance.

In the present paper, a statistical-dynamical scheme was developed for water table prediction under stream–aquifer interactions in an arid region; it consisted of a differential dynamical model based on Darcy's law, a stage-discharge function derived from fitted rating curves (Kazama *et al.*, 2005), and a parameter calibration method (the Shuffled Complex Evolution method developed at the University of Arizona or SCE-UA; Duan *et al.*, 1992). The proposed scheme was validated by sensitivity experiments and section observation in the lower reaches of the Tarim River.

METHODOLOGY

Differential dynamical model

For hydraulically connected stream–aquifer systems, the resulting exchange flow is a function of the difference between the river stage and aquifer head (Sophocleous, 2002). A simple approach to estimate the exchange is to consider it as being controlled by the same mechanism as leakage through a semi-impervious stratum in one dimension (Rushton and Tomlinson, 1979). This mechanism, based on Darcy's law, where flow is a direct function of the hydraulic conductivity and head difference, can be expressed as

$$Q = \frac{kS(h_i - h_j)}{l}, \tag{1}$$

where h_i and h_j are hydraulic head for grid cells i and j respectively, l is the distance between the grid cells i and j, Q is the lateral flow between the grid cells (positive for i towards j, and negative for j towards i), and k and S are the average hydraulic conductivity and cross-sectional area between them respectively.

It is assumed that there are n grid cells perpendicular to the direction of the river channel (Figure 1c), and all grid cells have the same lengths and widths. If the major water table gradient is perpendicular to the direction of river channel and the exchange between the saturated and unsaturated zones of the arid region is neglected due to the deep water table, then the water balance equations for groundwater in each grid cell can be written according to the mechanism described in Equation (1) as follows:

$$s_y \frac{dh_j}{dt} l^2 = \frac{k_{j-1,\ j} S_{j-1,\ j} (h_{j-1} - h_j)}{l} + \frac{k_{j,\ j+1} S_{j,\ j+1} (h_{j+1} - h_j)}{l} \quad (j = 1, \cdots, n), \tag{2}$$

where s_y[L/L] is the specific yield; $h_j (j = 1, \cdots, n)$[L] is the water table elevation for the jth grid cell and h_0 is the river elevation; $k_{j-1,\ j}$[L/T] and $S_{j-1,\ j}$[L^2] are the average hydraulic conductivity and cross section area between the $j-1$th and jth grid cells respectively; and l[L] is the distance between the adjacent grid cells.

Let $T_j = k_{j,\ j+1} S_{j,\ j+1} / (l^3 s_y)$ $(j = 0, \cdots, n)$ be the flow conductance coefficients [T^{-1}], and the right boundary flux be zero for the nth grid cell (Figure 1c), then Equation (2) can be written as

$$\begin{cases} \dfrac{dh_1(t)}{dt} = T_0(h_0(t) - h_1(t)) + T_1(h_2(t) - h_1(t)), \\ \dfrac{dh_j(t)}{dt} = {}^{T_{j-1}(h_{j-1}(t) - h_j(t)) +}_{T_j(h_{j+1}(t) - h_j(t))} \quad (j = 2, \cdots, n-1), \\ \dfrac{dh_n(t)}{dt} = T_{n-1}(h_{n-1}(t) - h_n(t)), \end{cases}$$

which can be written in vector notation:

$$\begin{cases} \dfrac{d\mathbf{X}(t)}{dt} = \mathbf{A}\mathbf{X}(t) + \mathbf{f}(t), \\ \mathbf{X}(t_0) = \mathbf{X}_0, \end{cases} \tag{3}$$

where $\mathbf{X}(t) = (h_1(t), \cdots, h_n(t))'$, $\mathbf{f}(t) = (T_0(t)h_0(t), 0, \cdots, 0)'$, $\mathbf{X}_0$ is the vector that consists of initial water table elevations, and

$$\mathbf{A} = \begin{pmatrix} -(T_0 + T_1) & T_1 & \cdots & 0 \\ T_1 & -(T_1 + T_2) & \ddots & \vdots \\ \vdots & \ddots & \ddots & T_{n-1} \\ 0 & \cdots & T_{n-1} & -T_{n-1} \end{pmatrix}.$$

Therefore, the problem of water table prediction under groundwater–river interactions has been reduced to an initial value problem of the differential Equation (3). Let $\mathbf{\Phi}(t)$ be the fundamental solution matrix for the homogeneous equation of Equation (3), we obtain its analytic solution as follows:

$$\mathbf{X}(t) = \mathbf{\Phi}(t)\mathbf{\Phi}^{-1}(t_0)\mathbf{X}_0 + \int_{t_0}^{t} \mathbf{\Phi}(t)\mathbf{\Phi}^{-1}(s)\mathbf{f}(s)ds. \tag{4}$$

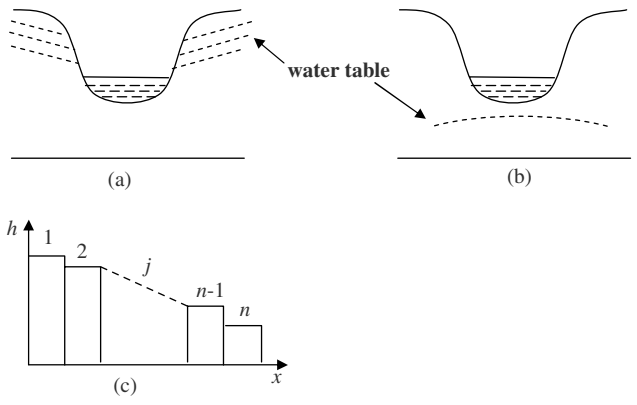

Figure 1. Possible situations for leakage between streams and aquifers, and the discrete grid cells. (a) For gaining stream; (b) for losing stream; and (c) for discrete grid cells

Stage-discharge function

Equation (4) can predict water table elevations at time t with the given river elevations over time (t_0, t). However, the river elevation data were not always available in this study, which can be calculated according to the stage-discharge function expressed as follows (Xu *et al.*, 2004):

$$Q(t) = a(H(t) - H_0)^b,$$

where $Q(t)$ is the discharge, $H(t)$ is the river elevation, H_0 is the river bed elevation, and a and b are the parameters. This is the most common way of describing the relationship between discharge and river elevation at

DOI: 10.1002/hyp

a gauging station. As the parameters have been calibrated by observed river elevation and discharge data, the river elevation can be estimated by discharge simultaneously:

$$H(t) = H_0 + (Q(t)/a)^{1/b}. \quad (5)$$

Model simplification and its coupling with the calibration method SCE-UA

As the range of the study domain was about 1 km (the range for the response of groundwater to water release; Chen *et al.*, 2004), we neglected the spatial heterogeneity of the groundwater flow conductance coefficients, i.e. $T_j = T_1 (j = 2, \cdots, n)$. The prognostic model described in Equation (3) has only two parameters (T_0 and T_1) to be calibrated. The flow conductance coefficients T_0 and T_1 are dependent on the size of the discrete grid cells, and are parameterized particularly.

Similar to Fan *et al.* (2007), we assumed that the hydraulic conductivity for groundwater flow decayed exponentially with depth,

$$K = K_1 \exp(-z/f),$$

where K_1 is the groundwater hydraulic conductivity for the surface soil ($z = 0$) and f is the e-folding length, which is parameterized as the following hyperbolic equation (Fan *et al.*, 2007),

$$f = \frac{120}{1 + 150\beta}, \quad \text{for} \quad \beta \leq 0{\cdot}16;$$
$$f = 5 \text{ m}, \quad \text{for} \quad \beta > 0{\cdot}16; \quad (6)$$

where β is the terrain slope. If the water table depth is d[L], the groundwater flow conductance coefficients T_1 can be written as

$$T_1 = l \int_d^\infty K dz/(l^3 s_y) = l \int_d^\infty K_1 \exp(-z/f) dz/(l^3 s_y) = K_1 f e^{-d/f}/(l^2 s_y).$$

Considering that $d/f < 0{\cdot}1$ in our case, we obtained

$$T_1 \approx K_1 f/(l^2 s_y). \quad (7)$$

Let K_0 be the hydraulic conductivity at the river bed and w be the river width, then the flow conductance coefficient T_0 with respect to groundwater–river exchange can be written as

$$T_0 = K_0 wl/(l^3 s_y) = K_0 w/(l^2 s_y). \quad (8)$$

It follows from Equations (7) and (8) that, once the parameters K_0 and K_1 are calibrated, Equation (4) can be used to predict the water table depths in different spatial resolution with an initial condition.

To calibrate the differential model, the SCE-UA algorithm (Duan *et al.*, 1992; Duan *et al.*, 1994) is adopted, which does not require the derivatives of the objective function, and can avoid being trapped by small pits and bumps on the function surface. SCE-UA is based on a synthesis of four concepts: (1) combination of deterministic and probabilistic approaches; (2) systematic evolution of a complex of points spanning the parameter space in the direction of global improvement; (3) competitive evolution; and (4) complex shuffling.

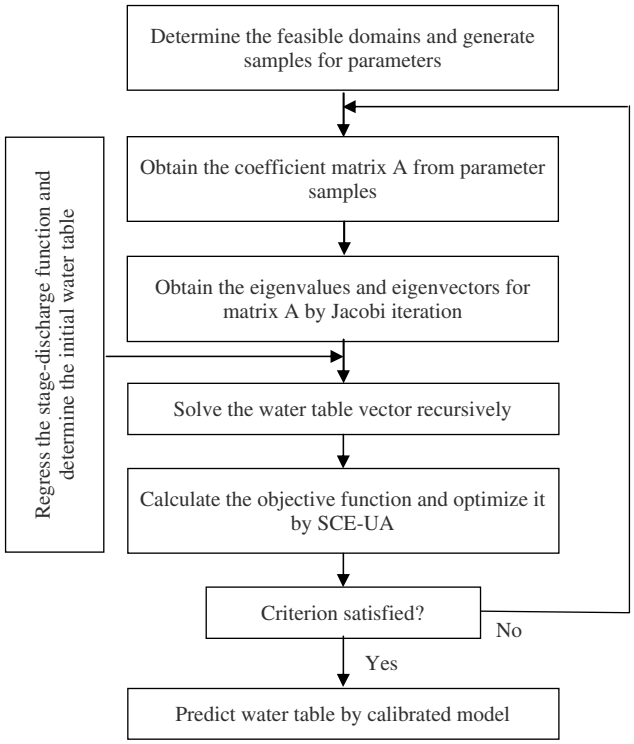

Figure 2. Schematic representation of the statistical–dynamical approach for water table prediction

The evolution of the proposed statistical-dynamical scheme, including differential model, stage-discharge function, and SCE-UA method (shown in Figure 2), can be manipulated as follows:

1. Regress the stage-discharge function based on the river elevation and discharge observations and determine the initial water table elevation by linear interpolation.
2. Determine the feasible domain for the parameters to be calibrated and obtain the initial guess for the coefficient matrix $\boldsymbol{A}$ by using initial parameters.
3. Obtain the eigenvalues and eigenvectors for matrix $\boldsymbol{A}$ by using Jacobi method iteratively.
4. Solve the water table vector $X(t_n)$ by

$$\boldsymbol{X}(t_n) = \boldsymbol{V} \begin{pmatrix} e^{\lambda_1 \Delta t} & \cdots & 0 \\ \vdots & \ddots & \vdots \\ 0 & \cdots & e^{\lambda_n \Delta t} \end{pmatrix} \boldsymbol{V}' \boldsymbol{X}(t_{n-1}) + \boldsymbol{V} \begin{pmatrix} \frac{e^{\lambda_1 \Delta t} - 1}{\lambda_1} & \cdots & 0 \\ \vdots & \ddots & \vdots \\ 0 & \cdots & \frac{e^{\lambda_n \Delta t} - 1}{\lambda_n} \end{pmatrix} \boldsymbol{V}' \mathbf{f}(t_{n-1})$$

recursively, where the column vectors for matrix $\boldsymbol{V}$ are the eigenvectors of matrix $\boldsymbol{A}$, and $\lambda_j (j = 1, \cdots, n)$ are the eigenvalues of matrix $\boldsymbol{A}$.

DOI: 10.1002/hyp

5. Determine the value of objective function by calculating the mean absolute error from the observed and simulated water table.
6. Calibrate the parameters using the SCE-UA method.
7. Predict the water table by the calibrated model.

MODEL SENSITIVITY

To test the sensitivities of model parameters, the river bed hydraulic conductivity K_0 and groundwater hydraulic conductivity K_1, the synthetic series of the river discharge and the related river elevation described in Equation (5) with $a = 6{\cdot}4$, $b = 1{\cdot}7$, and the initial water table elevations following $y = -0{\cdot}001x + 828{\cdot}3$ were applied to the differential model in Equation (4). Two sensitivity experiments with grid cell number $n = 100$ were conducted. The first experiment was with the parameters $K_0 = 3$, 6, 12, and 24 m/day, and $K_1 = 4$ m/day; and the second one was with the parameters $K_1 = 2$, 4, 8, and 16 m/day, and $K_0 = 7{\cdot}4$ m/day. The river elevation and the simulated water table elevations are shown in Figure 3. The lines on the Figure 3a–h show the water table level in each of the 100 grid cells, where the highest values refer to cells closest to the river. It follows for the first experiment (Figure 3a–d) that the elevated extent for water table increased as the river bed hydraulic conductivity increased, and the effects of K_0 on the variations of simulated water table were more obvious for the grid cells near the river (the upper part of the time series set) than those far from the river (the lower part of the time series set). It follows for the second experiment (Figure 3e–h) that the difference in water table elevations for grid cells with different distances from the river channel decreased as the groundwater hydraulic conductivity increased. This is because the increased groundwater hydraulic conductivity reduces the response time of different grid cells. In short, the differential dynamical model was validated by the sensitivity experiments and was used to investigate the response of the water table to river recharge in the consequent study.

MODEL VALIDATION

Data

The study area is located between Daxihaizi Reservoir and Taitema Lake in the lower reaches of the Tarim River (Figure 4), and has annual precipitation of 17·1–42·0 mm (Chen *et al.*, 2010). The data for river discharge, river elevation, and water table are collected from the EWCP. Nine cross sections between the Daxihaizi Reservoir and Taitema Lake were used to monitor the ecological effects of the water release (Figure 4). The EWCP was implemented in May 2000; the information on the first seven water releases is shown in Table I. The first water release lasted 61 days and the discharge at the Daxihaizi Reservoir was $1{\cdot}0 \times 10^8$ m^3. After the first release, the water head arrived at Kaerdayi section, about 102 km from the reservoir. After the second release, the water head arrived at Alagan section, about 146 km from the reservoir, and the discharge was $2{\cdot}2 \times 10^8$ m^3. The water head arrived at the Taitema Lake on 2 November 2001 and 4 October 2002 during the third and fourth releases, which resulted in 4·5 and 16 km^2 discharge areas in Taitema Lake, respectively. During the first seven water releases, the total discharge at the Daxihaizi Reservoir was $2{\cdot}25 \times 10^9$ m^3.

The Yingsu section is the third monitoring section downstream on the Tarim River, and is 60 km from the Daxihaizi Reservoir. The distances between the river bank and the four monitoring wells were 150, 300, 500, and 750 m, respectively (Figure 4). The river discharge and water table data were available for each water release, but the river elevation data were only available for releases 5–7. The river discharges were observed daily during the water release, and the water table only every 5 days or once a month. The water table depths were about 8–10 m before the first water release, and about 4–6 m after the seventh water release.

Regressing the river elevation from discharge

Before applying the numerical model mentioned above at the Yingsu section in the lower reaches of Tarim River, we obtained the river elevation data. The observed river elevations and discharges are shown in Figure 5 (the dotted line), indicating obvious exponential relationships between discharge and river elevation as described in Equation (5). Through regression, the fitted stage-discharge function can be expressed as follows:

$$H(t) = 832{\cdot}608 + (Q(t)/6{\cdot}4203)^{0{\cdot}5877},$$

which is also shown in Figure 5 (the solid line). The mean absolute error and correlation coefficient for the regressed function were 0·067 and 0·99 m respectively.

Calibration and validation

The data for the second water release were used to calibrate the model, and the beginning day for integrating the model was 16 November 2000 (the first available observation record). The linear regression function for the initial water table elevation is

$$y = -0{\cdot}0011x + 828{\cdot}2477,$$

where x is the distance (m) between the river bank and the calculation node and y is the water table elevation (m). The terrain slope β and its relevant e-folding length f from Equation (6) were set at 0·0011 and 103 m respectively. We set the specific yield $s_y = 0{\cdot}2$, river width $w = 10$ m, and the size of each grid cell $l = 10$ m. The parameters for river bed hydraulic conductivity K_0 and groundwater hydraulic conductivity K_1 calibrated by the SCE-UA method were 7·413 and 4·006 m/day respectively. The observed and simulated water table elevations and observed discharge and simulated river elevation from mid-November 2000 through mid-February

DOI: 10.1002/hyp

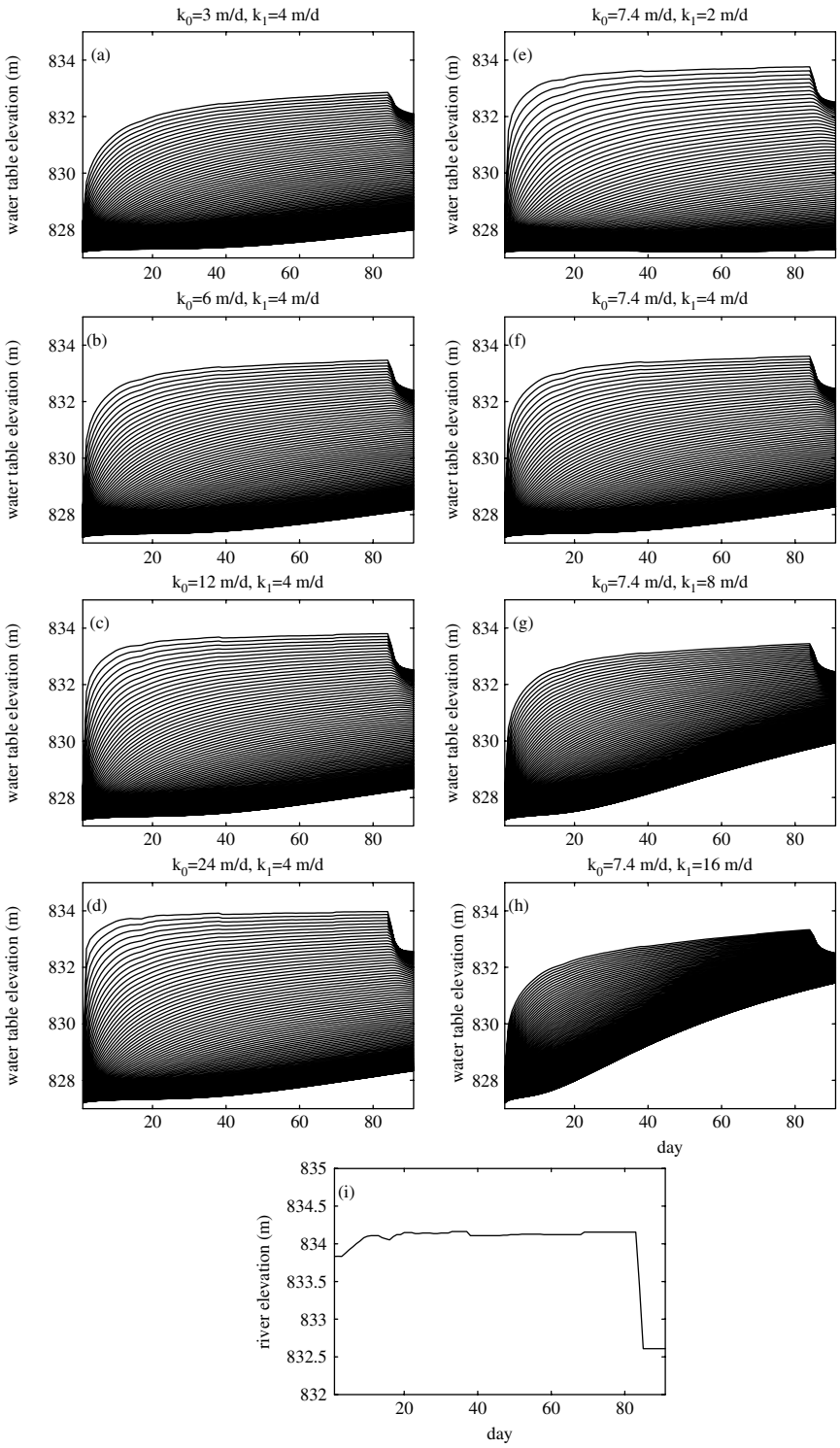

Figure 3. Sensitivities of the river bed hydraulic conductivity K_0 and groundwater hydraulic conductivity K_1. (a)–(d) are the time series of the simulated water table elevations for 100 grid cells in the first sensitivity experiment, (e)–(h) are the time series for the second experiment, (i) is the river elevation

2001 are shown in Figure 6. The systematic bias (ME), mean absolute error (MAE), root mean squared error (RMSE), and correlation coefficient (CC) were −0·170, 0·206, 0·321, and 0·985 m respectively.

We used the numerical model with calibrated parameters to estimate the spatiotemporal distribution of water table elevation near the river (Figure 7). Under the conditions of the water release, the elevated water table differed in different locations. The water table was elevated by 5·352 and 1·017 m for the nearest and farthest grid cells from the river bank respectively. The response speed of the water table to the discharge decreased from the grid cells nearby to those far from the river, and the elevation rates varied at 0·011–0·047 m/day. Owing to the various response speeds, the water table still rose for grid cells far from the river, though the river discharges

DOI: 10.1002/hyp

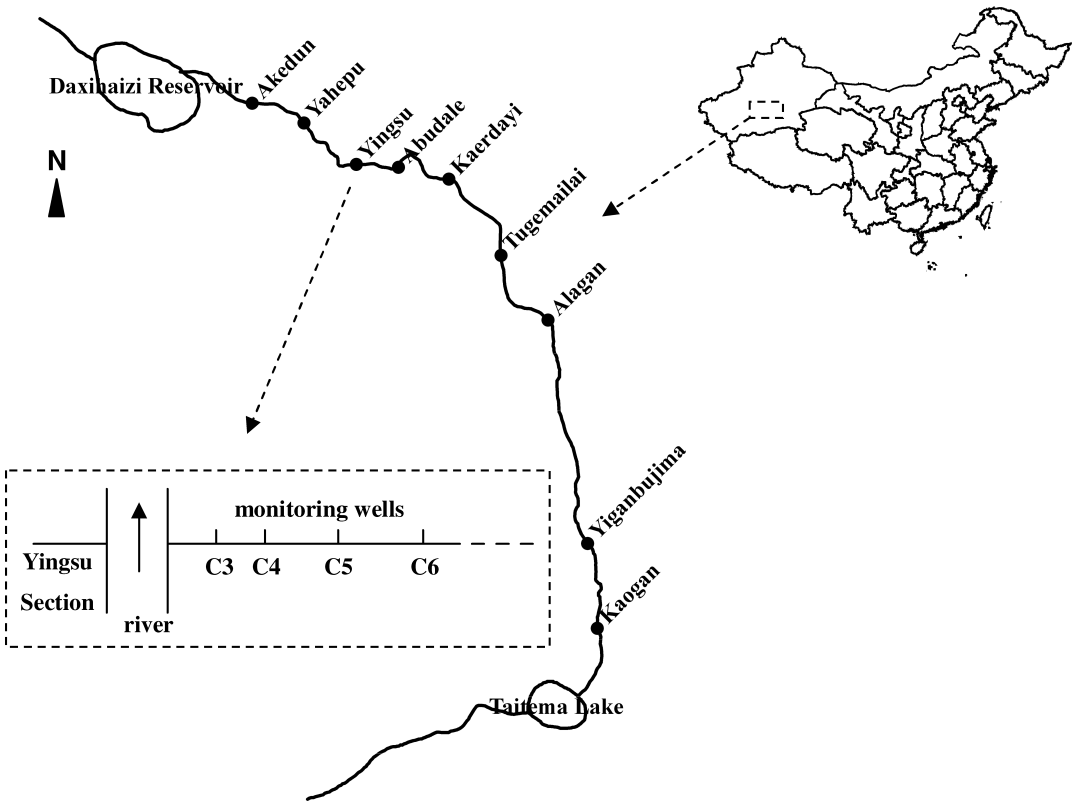

Figure 4. Locations of cross sections between the Daxihaizi Reservoir and Taitema Lake at the lower reaches of Tarim River, and the monitoring wells at Yingsu section

ceased during the last 7 days, while the water table decreased a little for grid cells near the river.

To validate the calibrated model, the model combined with discharge observation was adopted to predict the water table variations from the third to the seventh water releases. Figure 8 shows the validation results and Table II lists the average statistics of the four monitoring wells. The best results for ME, MAE and RMSE were in the third water release (Figure 8, left column), and the worst results for MAE and RMSE in the sixth release (Figure 8, the fourth column). The range of water table fluctuation seemed to correlate with the amount of discharge. The discharges for the fourth and fifth water releases (Figure 8f, k) were larger than those for the sixth and seventh (Figure 8p, u), and the water table fluctuation for the former (Figure 8g–j and l–o) were larger than those for the latter (Figure 8q–t and v–y).

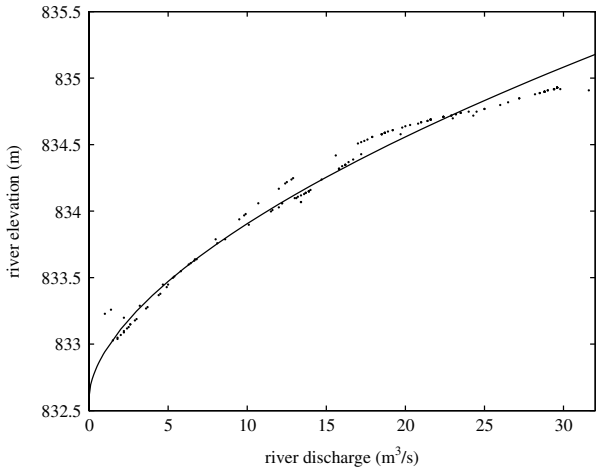

Figure 5. The relation between the observed discharge and river elevation (the dotted line) and the fitted rating curve (solid line)

Table I. The information for the first seven water releases

Water release	Begin date (year/ month)	End date (year/ month)	Amount ($10^8 m^3$)	Water head reached	Distance from reservoir (km)
1	2000/2005	2000/2007	0·98	Kaerdayi	102
2	2000/2011	2001/2002	2·20	Alagan	146
3	2001/2004	2001/2011	3·81	Taitema	321
4	2002/2007	2002/2011	2·93	Taitema	321
5	2003/2003	2003/2011	3·40	Taitema	321
6	2004/2004	2004/2011	3·50	Taitema	321
7	2005/2005	2005/2010	2·80	Taitema	321

The detailed simulation statistics for each well during each water release are shown in Figure9. The simulation results were more reliable for wells C3 and C4 than for C5 and C6, especially for the sixth and seventh water releases. The standard deviations of the simulated water table elevations (σ_s) from the third to fifth water releases were within the interval (0, $2\sigma_o$), and the correlation coefficients were $\geq$0·7. However, only 50% of the σ_s were in the interval ($0{\cdot}75\sigma_o$, $1{\cdot}25\sigma_o$), which indicates that the proposed method had some deficiency in capturing the amplitude of the variations of the water table.

DOI: 10.1002/hyp

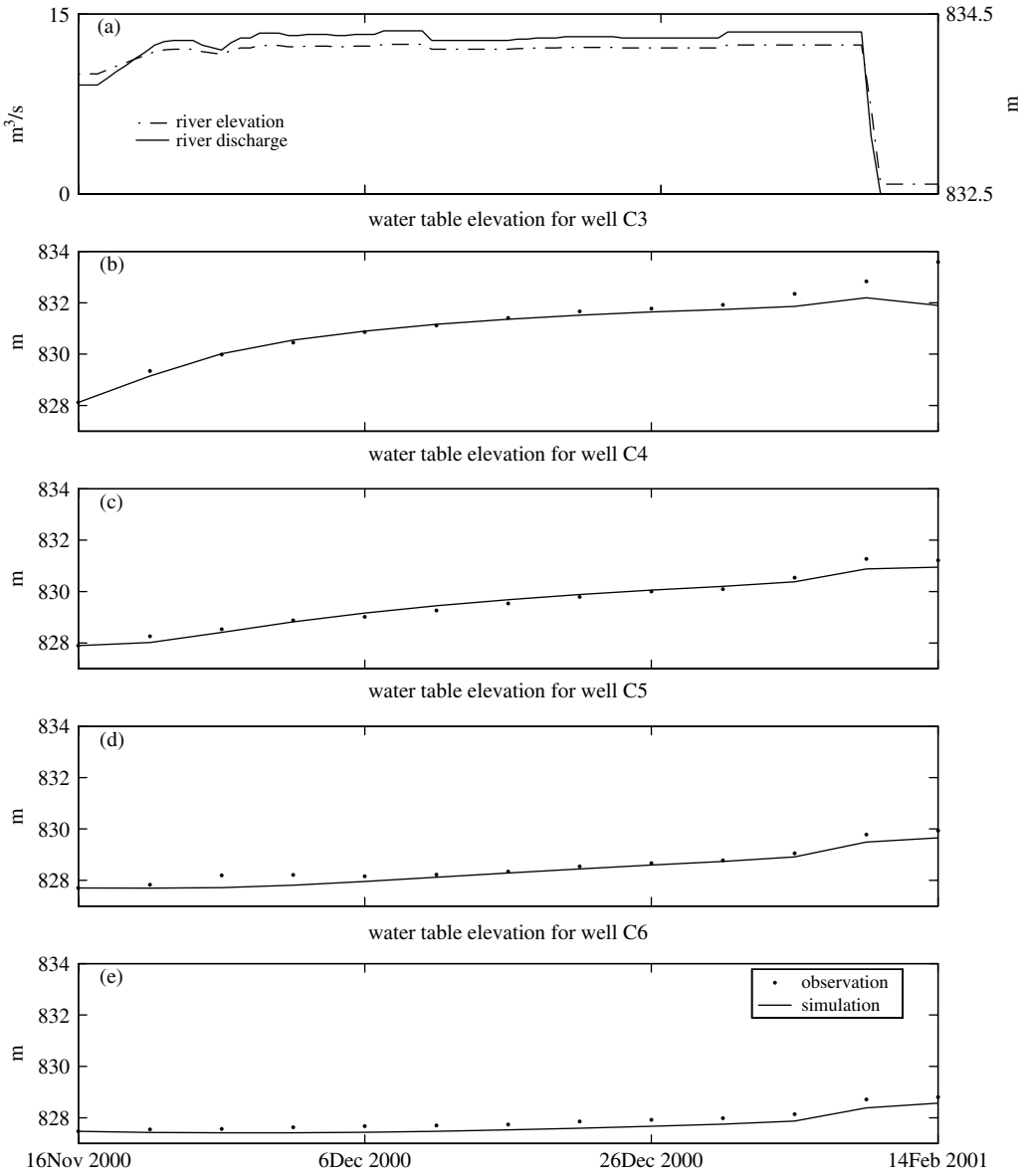

Figure 6. Time series for observed river discharge (a, solid line), estimated river elevation (a, dashed line), and observed and simulated water table elevations (b–e). (b), (c), (d), and (e) are for wells C3, C4, C5, and C6 respectively

CONCLUSIONS AND DISCUSSIONS

In arid regions, such as the Tarim River basin, the natural percolation through soil that reaches the water table is usually small, given the distance to cross and the dryness of the soil. Therefore, an important source of groundwater recharge is transmission losses in streams, and more generally in the hydrographic channel network (Dages *et al*., 2008). Without primary recharge from the rivers, the water table declines to such a level that natural vegetation cannot survive in the lower reaches of the Tarim River. To provide water to the terrestrial ecosystem along the Tarim River, the EWCP was initiated in 2000. The water conveyance significantly lifted the water table and increased the vegetation coverage. Many eco-hydrologists have investigated the relationship between the water table depths and vegetation diversity (Chen *et al*., 2004, 2009; Hao *et al*., 2010), while in this work the relation between the river discharge and water table dynamics along the river has been studied, which is important for water resource management and ecosystem sustainment.

This paper presents a statistical-dynamical scheme to predict the water table under stream–aquifer interaction in arid regions by reducing it to an initial value problem of the differential equations based on Darcy's law. The input of the model, the river elevation, was calculated by a stage-discharge function derived from fitted rating curves, and the model parameters were automatically calibrated by the SCE-UA method. The sensitivities of the model parameters were tested by synthetic experiments, which showed the ability of the proposed scheme to predict the water table under different conditions. The fitted rating curve reasonably represented the stage-discharge relation, and the MAE and CC for the regression were 0·067 and 0·99 m respectively. The calibration and validation results in the lower reaches of

DOI: 10.1002/hyp

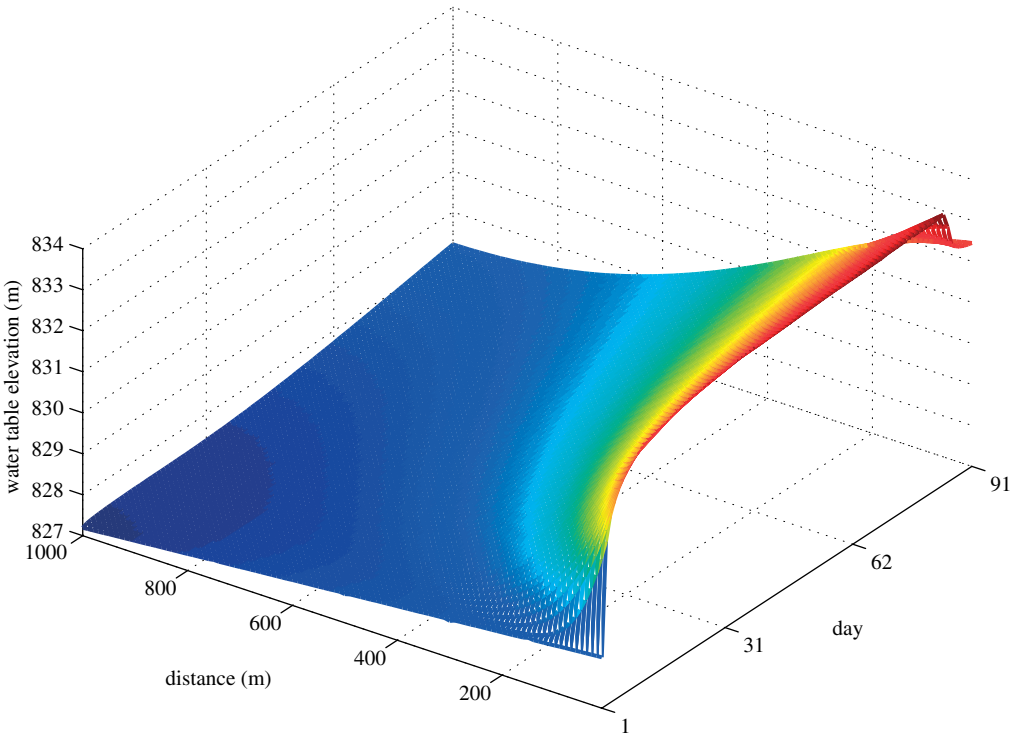

Figure 7. Spatial and temporal distribution of the simulated water table depths near the river bank during the second water release

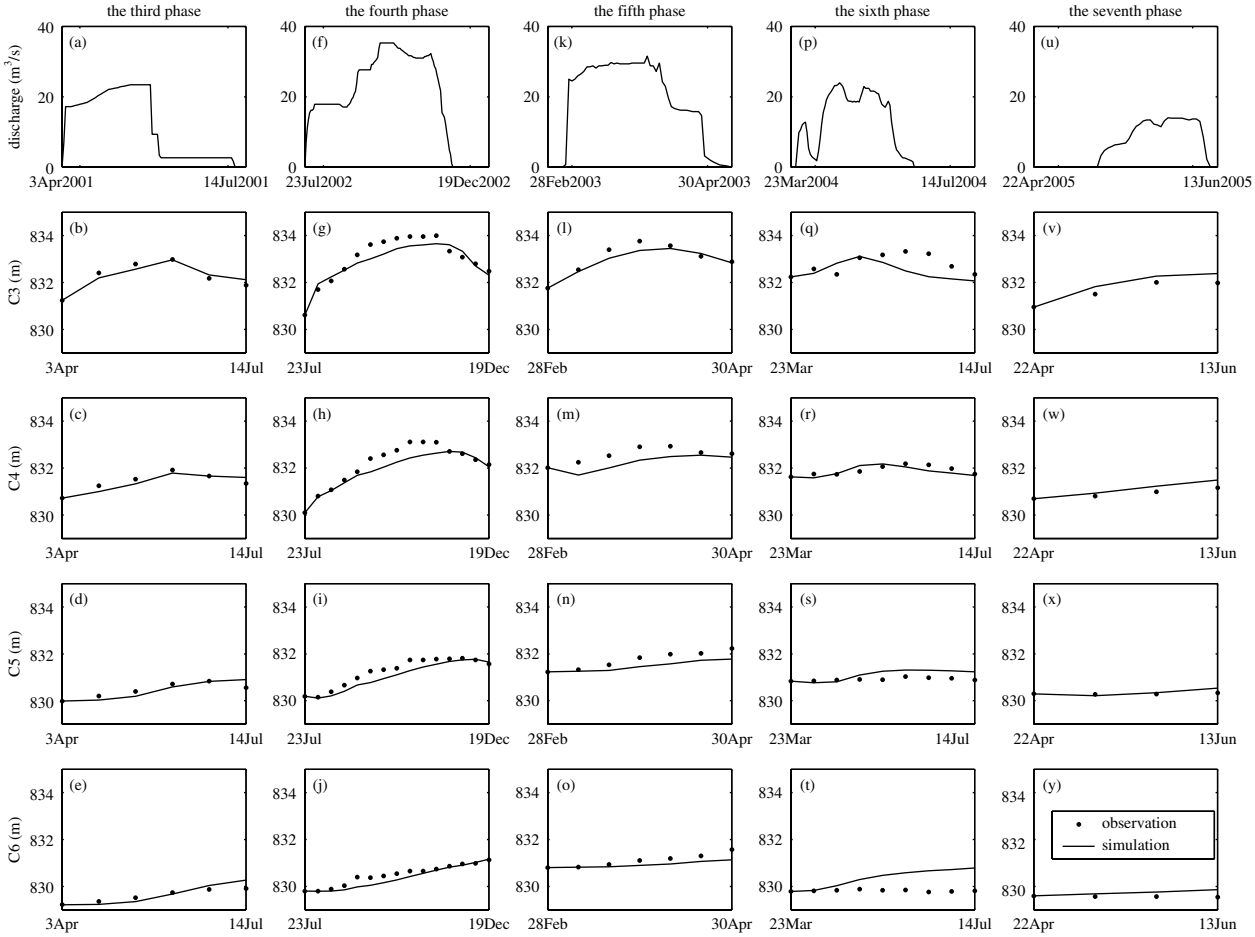

Figure 8. Observed river discharge (m^3/s, top row), observed (dotted line) and simulated (solid line) water table elevation (m). The rows from the second to the fifth are for wells C3, C4, C5, and C6 respectively. The columns from left to right are for the third to seventh water release respectively

DOI: 10.1002/hyp

the Tarim River indicate that the statistical-dynamical scheme simulated the water table with consideration of stream–aquifer interaction accurately when properly calibrated. The simulation results also showed that the rise in the water table due to the water conveyance varied 1–5 m in a region that was <1 km from the river bank. The rapid decrease trend for the water table rise suggested that the effects of the water conveyance on the groundwater level and hence on the vegetation were limited to a small region along the river, and multiple-channel water conveyance is needed to maintain the ecosystem and save the surface water.

As noted by Sophocleous (2002), the frontier in groundwater-surface water interaction is the near-channel and in-channel exchange of water, solutes, and energy; an understanding of these processes is the key to evaluating the ecological structure of stream systems and their management. To describe the water exchange processes between the stream and aquifer, numerical models have been widely used. However, their primary limitation is the difficulty of spatially defining the hydraulic properties and spatial heterogeneities of a stream bed, which control the interactions between surface water and the groundwater system. Statistical models can avoid the data scarcity problem to some extent, but even a simple time-series model has many uncertainties (Yuan *et al*., 2009). The present work took advantage of the numerical formulas and statistical techniques and produced an acceptable simulation. The water table vectors are written in the analytical form and solved numerically using the Jacobi iteration method, the hydraulic conductivities are parameterized by an empirical equation and calibrated by the SCE-UA optimization algorithm, and the stage-discharge function is regressed on the basis of river elevation and discharge observations. Although there are some simple hypotheses that need further validation, the present paper shows the potential for combining numerical modelling with statistical techniques in predicting water table under stream–aquifer interaction.

However, there are still a number of possible improvements to the proposed scheme as follows: (1) some vegetation roots are shallower than the water table and the available soil water in the root zone affects the growth of vegetation, therefore, groundwater–soil water interaction should be considered in the model; the recharge flux at the water table interface may provide the connection between the saturated and unsaturated vadose zone (Liang and Xie, 2003); (2) besides the coupling with the unsaturated zone, groundwater–vegetation interactions should also be taken into account, especially for the regions with deep-rooted vegetation or shallow water table; the vegetation transpires groundwater during the daytime (the groundwater evapotranspiration can be approximately 10% of total evapotranspiration; Yeh and Famiglietti, 2009), while hydraulic redistribution enables the movement of moisture from the upper to deeper soil layers during the nighttime in the wet season (Amenu and Kumar, 2008), which recharges groundwater; and (3) the connection of discharge between different cross sections needs to be parameterized to provide more precise stream stages, because the stream–aquifer seepage flows are driven by the head difference at the interface of two systems. Inaccuracies in the determination of stream stages on the seepage face would affect seepage fluxes and groundwater recharge rate. Further work will focus on coupling this scheme with the land surface model to account for the interactions and connections mentioned above.

Table II. Statistics for the calibration and validation[a]

Water release	Simulation days	Observation days	ME	MAE	RMSE	CC
2	91	13	−0·170	0·206	0·321	0·985
3	103	6	−0·015	0·141	0·179	0·986
4	150	15	−0·183	0·225	0·293	0·982
5	62	7	−0·224	0·232	0·296	0·973
6	114	9	0·097	0·325	0·441	0·943
7	53	4	0·159	0·165	0·213	0·989

[a] ME is the systematic bias, MAE is the mean absolute error, RMSE is the root mean squared error, and CC is the correlation coefficient.

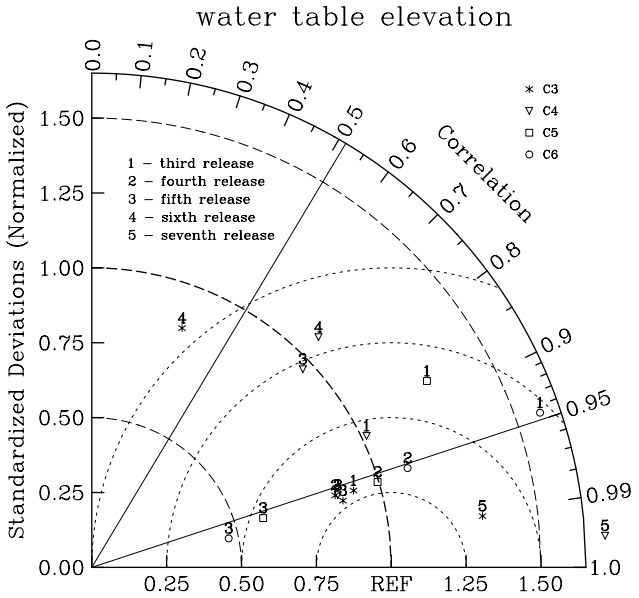

Figure 9. Statistics of the estimated water table elevations for wells C3, C4, C5, and C6 from the third to the seventh water release. The radial distance from the origin to the letters is the standard deviation of the simulated water table elevation (σ_s) normalized by the standard deviation of observations (σ_o) and the azimuthal position of the letters is the linear correlation between simulated and observed water table elevation

ACKNOWLEDGEMENTS

The authors would like to thank Prof. Yaning Chen for providing the related data collected at the Yingsu section and constructive discussions on this work and Feng Chen for constructive discussions on figure drawing. This manuscript benefited significantly from the comments and suggestions of the editor N E (Jake) Peters and two anonymous reviewers. This study was

supported by the Knowledge Innovation Project of Chinese Academy of Sciences under Grant Nos. KZCX2-YW-217 and KZCX2-YW-126-2, the National Basic Research Program under the Grant Nos. 2009CB421407 and 2005CB321703, and the National Natural Science Foundation of China under grant 40821092.

REFERENCES

Amenu GG, Kumar P. 2008. A model for hydraulic redistribution incorporating coupled soil-root moisture transport. *Hydrology and Earth System Sciences* **12**: 55–74.

Anyah RO, Weaver CP, Miguez-Macho G, Fan Y, Robock A. 2008. Incorporating water table dynamics in climate modeling: 3. Simulated groundwater influence on coupled land-atmosphere variability. *Journal of Geophysical Research* **113**: D07103, DOI: 10.1029/2007JD009087.

Bauer P, Gumbricht T, Kinzelbach W. 2006. A regional coupled surface water/groundwater model of the Okavango Delta, Botswana. *Water Resources Research* **42**: W04403, DOI: 10.1029/2005WR004234.

Brolsma RJ, Bierkens MFP. 2007. Groundwater-soil water-vegetation dynamics in a temperate forest ecosystem along a slope. *Water Resources Research* **43**: W01414, DOI: 10.1029/2005WR004696.

Chen XH. 2007. Hydrologic connections of a stream-aquifer-vegetation zone in south-central Platte River valley, Nebraska. *Journal of Hydrology* **333**: 554–568.

Chen X, Chen XH. 2003. Stream water infiltration, bank storage, and storage zone changes due to stream-stage fluctuations. *Journal of Hydrology* **280**: 246–264.

Chen Y, Chen Y, Xu C, Ye Z, Li Z, Zhu C, Ma X. 2010. Effects of ecological water conveyance on groundwater dynamics and riparian vegetation in the lower reaches of Tarim River, China. *Hydrological Processes* **24**: 170–177.

Chen X, Hu Q. 2004. Groundwater influences on soil moisture and surface evaporation. *Journal of Hydrology* **297**: 285–300.

Chen YN, Zhang XL, Li WH, Zhang YM. 2004. Analysis on the ecological benefits of the stream water conveyance to the dried-up river of the lower reaches of the Tarim River. *Science in China D* **47**: 1053–1064.

Dages C, Voltz M, Lacas JG, Huttel O, Negro S, Louchart X. 2008. An experimental study of water table recharge by seepage losses from a ditch with intermittent flow. *Hydrological Processes* **22**: 3555–3563.

Duan Q, Sorooshian S, Gupta VK. 1992. Effective and efficient global optimization for conceptual rainfall-runoff models. *Water Resources Research* **28**: 1015–1031.

Duan Q, Sorooshian S, Gupta VK. 1994. Optimal use of SCE-UA global optimization method for calibrating watershed models. *Journal of Hydrology* **158**: 265–284.

Fan Y, Miguez-Macho G, Weaver CP, Walko R, Robock A. 2007. Incorporating water table dynamics in climate modeling: 1. Water table observation and equilibrium water table simulations. *Journal of Geophysical Research* **112**: D10125, DOI: 10.1029/2006JD008111.

Feng Q, Endo KN, Cheng GD. 2001. Towards sustainable development of the environmentally degraded arid rivers of China—a case study from Tarim River. *Environmental Geology* **41**: 229–238.

Hao X, Li W, Huang X, Zhu C, Ma J. 2010. Assessment of the groundwater threshold of desert riparian forest vegetation along the middle and lower reaches of the Tarim River, China. *Hydrological Processes* **24**: 178–186.

Hu LT, Chen CX, Jiao JJ, Wang ZJ. 2007. Simulated groundwater interaction with rivers and springs in the Heihe river basin. *Hydrological Processes* **21**: 2794–2806.

Kazama S, Suzuki K, Sawamoto M. 2005. Estimation of rating curve parameters for sedimentation using a physical model. *Hydrological Processes* **19**: 3863–3871.

Liang X, Xie ZH. 2003. Important factors in land-atmosphere interactions: surface runoff generations and interactions between surface and groundwater. *Global and Planetary Change* **38**: 101–114.

Liang X, Xie ZH, Huang MY. 2003. A new parameterization for surface and groundwater interaction and its impact on water budgets with the variable infiltration capacity (VIC) land surface model. *Journal of Geophysical Research* **108**: 8613, DOI: 10.1029/2002JD003090.

Maxwell RM, Miller NL. 2005. Development of a coupled land surface and groundwater model. *Journal of Hydrometeorology* **6**: 233–247.

Miguez-Macho G, Fan Y, Weaver CP, Walko R, Robock A. 2007. Incorporating water table dynamics in climate modeling: 2. Formulation, validation, and soil moisture simulation. *Journal of Geophysical Research* **112**: D13108, DOI: 10.1029/2006JD008112.

Niu GY, Yang ZL, Dickinson RE, Gulden LE, Su H. 2007. Development of a simple groundwater model for use in climate models and evaluation with Gravity Recovery and Climate Experiment data. *Journal of Geophysical Research* **112**: D07103, DOI: 10.1029/2006JD007522.

Rushton KR, Tomlinson LM. 1979. Possible mechanisms for leakage between aquifers and rivers. *Journal of Hydrology* **40**: 49–65.

Sear DA, Armitage PD, Dawson FH. 1999. Groundwater dominated rivers. *Hydrological Processes* **13**(3): 255–276.

Sophocleous M. 2002. Interactions between groundwater and surface water: the state of the science. *Hydrogeology Journal* **10**: 52–67.

Wu RS, Shih DS, Li MH, Niu CC. 2008. Coupled surface and ground water models for investigating hydrological processes. *Hydrological Processes* **22**: 1216–1229.

Xu HL, Ye M, Song YD, Chen YN. 2007. The natural vegetation responses to the groundwater change resulting from ecological water conveyances to the lower Tarim River. *Environmental Monitoring and Assessment* **131**: 37–48.

Xu KQ, Zhang JQ, Watanabe M, Sun CP. 2004. Estimating river discharge from very high-resolution satellite data: a case study in the Yangtze River, China. *Hydrological Processes* **18**: 1927–1939.

Yang HW, Xie ZH. 2003. A new method to dynamically simulate groundwater table in land surface model VIC. *Progress in Natural Science* **13**: 819–825.

Yeh PJF, Eltahir EAB. 2005. Representation of water table dynamics in a land surface scheme, part I: model development. *Journal of Climate* **18**: 1861–1880.

Yeh PJF, Famiglietti JS. 2009. Regional groundwater evapotranspiration in Illinois. *Journal of Hydrometeorology* **10**: 464–478.

Yuan X, Xie ZH, Liang ML. 2008a. Spatiotemporal prediction of shallow water table depths in continental China. *Water Resources Research* **44**: W04414, DOI: 10.1029/2006WR005453.

Yuan X, Xie ZH, Liang ML. 2009. Sensitivity of regionalized transfer-function noise models to the input and parameter transfer method. *Hydrological Sciences Journal-des Sciences Hydrologiques* **54**(3): 639–651.

Yuan X, Xie ZH, Zheng J, Tian XJ, Yang ZL. 2008b. Effects of water table dynamics on regional climate: A case study over east Asian monsoon area. *Journal of Geophysical Research* **113**: D21112, DOI:10.1029/2008JD010180.